

# Lepton number violation and $h \rightarrow \gamma\gamma$ in a radiative inverse seesaw dark matter model

Guan-Nan Li,<sup>1</sup> Gang Guo,<sup>1</sup> Bo Ren,<sup>2</sup> Ya-Juan Zheng,<sup>3</sup> and Xiao-Gang He<sup>1,3,4,\*</sup>

<sup>1</sup>*INPAC, SKLPPC and Department of Physics,  
Shanghai Jiao Tong University, Shanghai, China*

<sup>2</sup>*Department of Physics, Shaoxing University, Shaoxing, Zhejiang, China*

<sup>3</sup>*CTS, CASTS and Department of Physics,  
National Taiwan University, Taipei, Taiwan*

<sup>4</sup>*Department of Physics, National Tsing Hua University, and  
National Center for Theoretical Sciences, Hsinchu, Taiwan*

(Dated: October 10, 2018)

## Abstract

We study phenomenological implications of a radiative inverse seesaw dark matter model. In this model, because neutrino masses are generated at two loop level with inverse seesaw, the new physics mass scale can be as low as a few hundred GeV and the model also naturally contain dark matter candidate. The Yukawa couplings linking the SM leptons and new particles can be large. This can lead to large lepton flavor violating effects. We find that future experimental data on  $\mu \rightarrow e\gamma$  and  $\mu - e$  conversion can further test the model. The new charged particles can affect significantly the  $h \rightarrow \gamma\gamma$  branching ratio in the SM. The model is able to explain the deviation between the SM prediction and the LHC data. We also study some LHC signatures of the new particles in the model.

PACS numbers: 12.60.Fr, 13.30.Ce, 95.35.+d, 14.80.Ec, 14.80.Fd

---

\*Electronic address: hexg@phys.ntu.edu.tw

## I. INTRODUCTION

Seesaw mechanism is one of the popular mechanisms[1–3] beyond the standard model (SM) which can provide some explanations why neutrino masses are small. Usually the seesaw scale is large making LHC study of the new physics scale difficult. The inverse seesaw mechanism[4] can lower the seesaw scale, because in this type of models the light neutrino masses are suppressed by higher powers of new scale beyond the SM. If the inverse seesaw mechanism is also achieved by radiative correction, the new scale can be even lower. Such low new physics scale can lead to large testable effects in various experiments. Recently models of this type have been proposed in which inverse seesaw mechanism is radiatively realized at two loop level[5]. This allows the new physics scale to be in the hundreds GeV range. To forbid tree and one loop level neutrino mass generation, new unbroken symmetries are introduced. The lightest new particles transforming non-trivially under the new symmetries are stable and can play the role of dark matter needed to explain about 23% of the energy budget of our universe[6].

In this paper we further study some phenomenologies in one of the promising models. The model we will study is the  $U(1)_D$  model discussed in Ref.[5]. There are several new particles in this model. The large Yukawa couplings linking the SM leptons and new particles in this model can have large lepton flavor violating(LFV) effects. Future experimental data on  $\mu \rightarrow e\gamma$  and  $\mu - e$  conversion can further test the model. The new charged particles can affect significantly the  $h \rightarrow \gamma\gamma$  branching ratio in the SM and the new contributions may be able to explain the deviation between the SM prediction and the LHC data. We now provide some details in the following.

## II. THE MODEL

The model is based on the  $SU(2)_L \times U(1)_Y$  SM electroweak gauge group with an unbroken global  $U(1)_D$  symmetry. The SM particles do not transform under the  $U(1)_D$  symmetry. New particles in this model are vectorlike leptonic  $SU(2)_L$  doublets  $D_{L,R}$ , two scalar singlets  $S$ ,  $\sigma$  and a scalar  $SU(2)_L$  triplet  $\Delta$ . Their SM and  $U(1)_D$  charges are as follows

$$D_{L,R} : (2, -1/2)(1), \quad S : (1, 0)(-1), \quad \sigma : (1, 0)(2), \quad \Delta : (3, -1)(2). \quad (1)$$

In the above the two numbers in the first and the second brackets are the  $SU(2)_L \times U(1)_Y$ , and the  $U(1)_D$  quantum numbers, respectively.

The renormalizable terms for Yukawa couplings  $L_D$  consistent with the symmetries of the model are

$$L_D = -\bar{L}_L Y_D D_R S - \bar{D}_L M D_R - \frac{1}{2} \bar{D}_L Y_L D_L^c \Delta - \frac{1}{2} \bar{D}_R^c Y_R D_R \Delta^\dagger + h.c. \quad (2)$$

The allowed renormalizable terms in the potential  $V_D$  are given by

$$V_D = -\mu_H^2 H^\dagger H + \lambda_H (H^\dagger H)^2 + \mu_S^2 S^\dagger S + \lambda_S (S^\dagger S)^2 + \mu_\sigma^2 \sigma^\dagger \sigma + \lambda_\sigma (\sigma^\dagger \sigma)^2 \\ + \mu_\Delta^2 \Delta^\dagger \Delta + \lambda_\Delta^\alpha (\Delta^\dagger \Delta \Delta^\dagger \Delta)_\alpha + \sum_{ij} \lambda_{ij} i^\dagger i j^\dagger j + (\mu_{S\sigma} S^2 \sigma + \lambda_{\Delta\sigma H} H \Delta \sigma^\dagger H + h.c.), \quad (3)$$

where the sum  $\sum_{ij}$  is over all possible  $i$  and  $j$ , and  $i$  to be one of the  $H$ ,  $S$ ,  $\sigma$  and  $\Delta$ . The allowed terms are

$$\lambda_{H\Delta}^\beta (H^\dagger H \Delta^\dagger \Delta)_\beta + \lambda_{H\sigma} (H^\dagger H \sigma^\dagger \sigma) + \lambda_{HS} (H^\dagger H S^\dagger S) \\ + \lambda_{\Delta S} (\Delta^\dagger \Delta S^\dagger S) + \lambda_{\Delta\sigma} (\Delta^\dagger \Delta \sigma^\dagger \sigma) + \lambda_{\sigma S} (\sigma^\dagger \sigma S^\dagger S). \quad (4)$$

In the above the indices  $\alpha$  and  $\beta$  indicate different ways of forming singlets. They are given by

$$(\Delta^\dagger \Delta \Delta^\dagger \Delta)_1 = \Delta_{ij}^* \Delta_{ij} \Delta_{kl}^* \Delta_{kl}, \quad (\Delta^\dagger \Delta \Delta^\dagger \Delta)_2 = \Delta_{ij}^* \Delta_{ik} \Delta_{kl}^* \Delta_{jl} \\ (\Delta^\dagger \Delta H^\dagger H)_1 = \Delta_{ij}^* \Delta_{ij} H_k^* H_k, \quad (\Delta^\dagger \Delta H^\dagger H)_2 = \Delta_{ij}^* \Delta_{kj} H_k^* H_i \quad (5)$$

If both  $S$  and  $\Delta$  develop non-zero vev's, the Lagrangian  $L_D$  will give the usual inverse seesaw masses to neutrinos. In that case there will be a Goldstone boson due to breaking of the global  $U(1)_D$  symmetry which may be problematic. To avoid the appearance of massless Goldstone boson in the theory, a possible approach is to keep the global symmetry to be exact and therefore no Goldstone boson emerges. This requires  $\mu_i^2$  to be all larger than zero. This also forbids the light neutrinos to have non-zero masses at tree level. However, Majorana neutrino masses can be generated at two loop level through the Feynman diagram shown in Fig.1.

Carrying out the loop integrals, one obtains neutrino mass matrix  $m_\nu$  in the bases where  $M$  is diagonal

$$m_\nu^{ij} = \frac{v_H Y_D^{ik} (\lambda_{\Delta\sigma H} \mu_{S\sigma} Y_L^{kl}) Y_D^{jl} v_H}{M_{kk}^2} \kappa_{kl}, \quad (6)$$

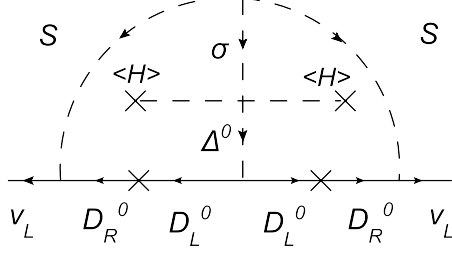


FIG. 1: Two loop Feynman diagram for neutrino mass generation.

where  $\kappa_{kl}$  is defined as

$$\kappa_{kl} = \delta_{kl} \frac{1}{2(4\pi)^4} \frac{1}{(1 - m_S^2/M_{kk}^2)^2} [g(m_{\phi_1}, m_S, m_S) - g(m_{\phi_1}, M_{kk}, m_S) - g(m_{\phi_1}, m_S, M_{kk}) + g(m_{\phi_1}, M_{kk}, M_{kk})]. \quad (7)$$

$$g(m_1, m_2, m_3) = \int_0^1 dx [1 + Sp(1 - \mu^2) - \frac{\mu^2}{1 - \mu^2} \log \mu^2]$$

with  $\mu^2 = \frac{ax+b(1-x)}{x(1-x)}$ ,  $a = \frac{m_2^2}{m_1^2}$ ,  $b = \frac{m_3^2}{m_1^2}$ .  $Sp(z)$  is the Spence function or the dilogarithm function

$$Sp(z) = - \int_0^z \frac{\ln(1-t)}{t} dt \quad (8)$$

In the above we have assumed that  $\sigma$  and the neutral component of  $\Delta$  have almost equal mass  $m_{\phi_1}$ .

There are candidates for dark matter in this model. The neutral heavy particles in  $D_{L,R}$  and  $\Delta$  have non-zero hypercharges and have problems to play the role of dark matter. The natural dark matter candidate field is  $S$ . It does not have a non-zero hypercharge and does not mix with any particles with hypercharge ( $\sigma$  mixes with  $\Delta$ ). As long as dark matter properties are concerned, this model is very similar to the real singlet (darkon) model[7] and therefore has similar dark matter properties[8, 9] and is identical to the complex scalar singlet model[10] with degenerate mass for the real and imaginary parts of  $S$ . The term  $S^\dagger S H^\dagger H$  is important for dark matter relic density and direct detection studies.

The Higgs boson  $h$  properties, its mass and its couplings to SM particles (fermions and gauge bosons), are the same as those in the SM at the tree level. The recent LHC data indicate that the mass is about 126 GeV[11] which can be applied to this model. It has been shown that the dark matter relic density and direct detection constraints can be simultaneously satisfied with appropriate dark matter mass. The range of a few tens of GeV for

dark matter mass is in trouble. However, dark matter mass about half of the Higgs mass or larger than 130 GeV is allowed[5]. In our later discussions, we will take  $m_S = 150$  GeV for illustration.

### III. NEUTRINO MASSES AND LFV

The formula in Eq.(7) determines whether the model is consistent with current data on neutrino mixing and masses[12]. In order to have at least two neutrinos with non-zero mass to be consistent with data, more than one generation of  $D_{L,R}$  are needed. We will assume that there are three of them. The mixing pattern is determined by two Yukawa couplings,  $Y_D$  and  $Y_L$ . With three  $D_{L,R}$ , they both are  $3 \times 3$  matrices. In our numerical calculations, we will assume that the flavor structure is determined by the Yukawa coupling  $Y_D$  with  $Y_D = y_D U_{PMNS} \hat{Y}_D$  with  $Y_L$  diagonal for both normal and inverted hierarchies for neutrino masses. In our later calculations we will use the central values from recent global fit data in Ref.[12] for neutrino mixing angles and mass squared differences for both normal and inverted hierarchies (NH and IH) for our discussions

$$\begin{aligned}
\sin^2 \theta_{12} &= 0.307_{-0.016}^{+0.018}(\text{NH, IH}); \sin^2 \theta_{23} = 0.386_{-0.021}^{+0.024}(\text{NH}), 0.392_{-0.022}^{+0.039}(\text{IH}); \\
\sin^2 \theta_{13} &= 0.0241 \pm 0.0025(\text{NH}), 0.0244_{-0.0025}^{+0.0023}(\text{IH}); \\
\delta m^2 &= m_2^2 - m_1^2 = (7.54_{-0.22}^{+0.26}) \times 10^{-5} \text{eV}^2(\text{NH, IH}); \\
|\Delta m^2| &= |m_3^2 - (m_2^2 + m_1^2)/2| = (2.43_{-0.1}^{+0.06}) \times 10^{-3} \text{eV}^2(\text{NH}), (2.42_{-0.11}^{+0.07}) \times 10^{-3} \text{eV}^2(\text{IH}); \\
\delta &= 194.4^\circ(\text{NH}), \quad 196.2^\circ(\text{IH}).
\end{aligned} \tag{9}$$

In the following we show two sets of model parameters which can fit known data for neutrinos and take them as bench mark values.

For the normal hierarchy, choosing  $\hat{Y}_D = \text{diag}(1, \sqrt{1.03}, \sqrt{1.77})$ ,  $y_D \times \lambda_{\Delta\sigma H} = 10^{-3}$ ,  $Y_L = \text{I} \times 10^{-2}$ ,  $\mu_{S\sigma} = 100 \text{GeV}$ ,  $m_{\phi_1} = 300 \text{GeV}$ ,  $m_S = 150 \text{GeV}$ ,  $M_{ii} = 500 \text{GeV}$ , we can get all the three neutrino mass  $3.39 \times 10^{-2} \text{eV}$ ,  $3.50 \times 10^{-2} \text{eV}$ ,  $5.98 \times 10^{-2} \text{eV}$ , respectively. These are consistent with data.

For inverted hierarchy case, we just need to replace  $\hat{Y}_D$  with  $\hat{Y}_D = \text{diag}(\sqrt{1.46}, \sqrt{1.48}, \sqrt{0.100})$ , with all the other parameters unchanged, the neutrino masses will be  $4.93 \times 10^{-2} \text{eV}$ ,  $5.01 \times 10^{-2} \text{eV}$ ,  $3.39 \times 10^{-3} \text{eV}$ , respectively. Again, these numbers are consistent with data.

For neutrino masses, the two parameters  $y_D$  and  $\lambda_{\Delta\sigma H}$  appear together, but for charged lepton LFV processes which happen at one loop level, they only depend on  $y_D$ . We will study how  $y_D$  is constrained by data from  $l_i \rightarrow l_j\gamma$  and  $\mu - e$  conversion.

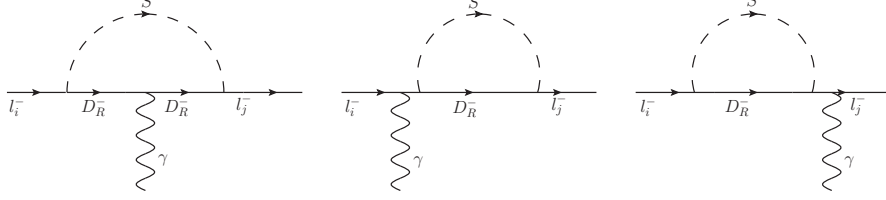


FIG. 2: Feynman diagrams for  $l_i \rightarrow l_j\gamma$ .

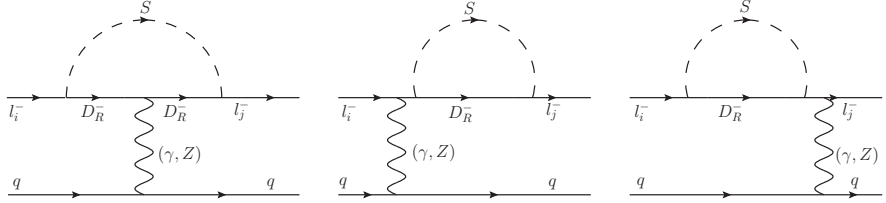


FIG. 3: Feynman diagrams for  $l_i - l_j$  conversion.

Radiative leptonic decay  $l_i \rightarrow l_j\gamma$  can occur at one loop level as shown in Fig.2. By attaching  $\gamma$ , and changing  $\gamma$  into  $Z$ , and then let  $\gamma$  and  $Z$  connect to quark, as shown in Fig.3,  $\mu - e$  conversion can be induced. For our case the Lagrangian responsible for  $l_i \rightarrow l_j\gamma$  and  $l_i - l_j$  conversion can be written as

$$\mathcal{L} = -\bar{l}_j\sigma^{\mu\nu}(A_{Lji}P_L + A_{Rji}P_R)l_i F_{\mu\nu} + \left[\sum_q eQ_q\bar{q}\gamma^\mu q\bar{l}_j B_{Lji}\gamma_\mu P_L l_i + H.c.\right], \quad (10)$$

and the functions  $A_{L,R}$  and  $B_L$  are given by

$$\begin{aligned} A_{Lji} &= Y_{Djk}Y_{Dki}^* \frac{e}{32\pi^2} \frac{1}{m_S^2} F_D\left(\frac{M_k^2}{m_S^2}\right) m_j, \quad A_{Rji} = \frac{m_i}{m_j} A_{Lji}, \\ B_{Lji} &= Y_{Djk}Y_{Dki}^* \frac{e}{16\pi^2} \frac{1}{m_S^2} G_D\left(\frac{M_k^2}{m_S^2}\right), \\ F_D(z) &= \frac{z^2 - 5z - 2}{12(z-1)^3} + \frac{z \ln z}{2(z-1)^4}, \\ G_D(z) &= \frac{7z^3 - 36z^2 + 45z - 16 + 6(3z-2)\ln z}{36(1-z)^4}. \end{aligned} \quad (11)$$

The LFV  $l_i \rightarrow l_j\gamma$  decay branching ratio is easily evaluated by

$$B(l_i \rightarrow l_j\gamma) = \frac{48\pi^2}{G_F^2 m_i^2} (|A_{Lji}|^2 + |A_{Rji}|^2). \quad (12)$$

The strength of  $\mu - e$  conversion is measured by the quantity,  $B_{\mu \rightarrow e}^A = \Gamma_{conv}^A / \Gamma_{capt}^A = \Gamma(\mu^- + A(N, Z) \rightarrow e^- + A(N, Z)) / \Gamma(\mu^- + A(N, Z) \rightarrow \nu_\mu + A(N + 1, Z - 1))$ . To obtain the conversion rate, one needs to convert the quarks in Eq.(11) into relevant nuclei. We will use the theoretical values compiled in Ref.[13]. We have[14]

$$\frac{B_{\mu \rightarrow e}^A}{B(\mu \rightarrow e\gamma)} = R_{\mu \rightarrow e}^0(A) \left| 1 + \frac{\tilde{g}_{LV}^{(p)} V^{(p)}(A)}{A_R D(A)} + \frac{\tilde{g}_{LV}^{(n)} V^{(n)}(A)}{A_R D(A)} \right|^2, \quad (13)$$

where

$$R_{\mu \rightarrow e}^0(A) = \frac{G_F^2 m_\mu^5}{192 \pi^2 \Gamma_{capt}^A} |D(A)|^2. \quad (14)$$

and

$$\tilde{g}_{LV}^{(p)} = 2g_{LV(u)} + g_{LV(d)}, \tilde{g}_{LV}^{(n)} = g_{LV(u)} + 2g_{LV(d)}, g_{LV(q)} = -4eQ_q m_\mu B_L. \quad (15)$$

The parameters  $D(A)$ ,  $V^{(p,n)}(A)$  are nuclei dependent quantities. Several of them are given in Ref.[13].

With the bench mark values for the model parameters fixed, the  $B(l_i \rightarrow l_j \gamma)$  and  $\mu - e$  conversion rate are all dependent on the coupling constant  $y_D$ . We now discuss the constraint on  $y_D$ .

Although  $\mu \rightarrow e\gamma$  has not been observed, there are stringent constraint on the upper limit of the branching ratio. The current upper limit is  $2.4 \times 10^{-12}$  at the 90% c.l.[15]. Experimental sensitivity will be improved. We take  $B(\mu \rightarrow e\gamma) = 1 \times 10^{-13}$ [16] as the near future improved MEG experimental sensitivity to constrain the parameter  $y_D$ . There are also bounds for the process of  $\tau \rightarrow \mu(e)\gamma$ . The current 95% c.l. experiment bounds are  $B(\tau \rightarrow e\gamma) < 3.3 \times 10^{-8}$ ,  $B(\tau \rightarrow \mu\gamma) < 4.4 \times 10^{-8}$ [17].

There are several measurements of  $\mu - e$  conversion on various nuclei. The best experimental bound is from Au nuclei with the 90% c.l. upper bound given by  $B_{\mu \rightarrow e}^{Au} < 7 \times 10^{-13}$ [18]. For Au, the relevant parameters determined by method I in Ref.[13] are given by:  $D(\text{Au}) = 0.189$ ,  $V^{(p)}(\text{Au}) = 0.0974$ ,  $V^{(n)}(\text{Au}) = 0.146$  and  $R_{\mu \rightarrow e}^0(\text{Au}) = 0.0036$ [13]. There are several planned experiments, such as Mu2E[19]/COMET[20] for  $\mu - e$  conversion using Al. The sensitivities are expected to reach  $10^{-16}$ [20]. For Al nuclei, the relevant parameters for our calculations are given by  $D(\text{Al}) = 0.0362$ ,  $V^{(p)}(\text{Al}) = 0.0161$ ,  $V^{(n)}(\text{Al}) = 0.0173$  and  $R_{\mu \rightarrow e}^0(\text{Al}) = 0.0026$ [13].

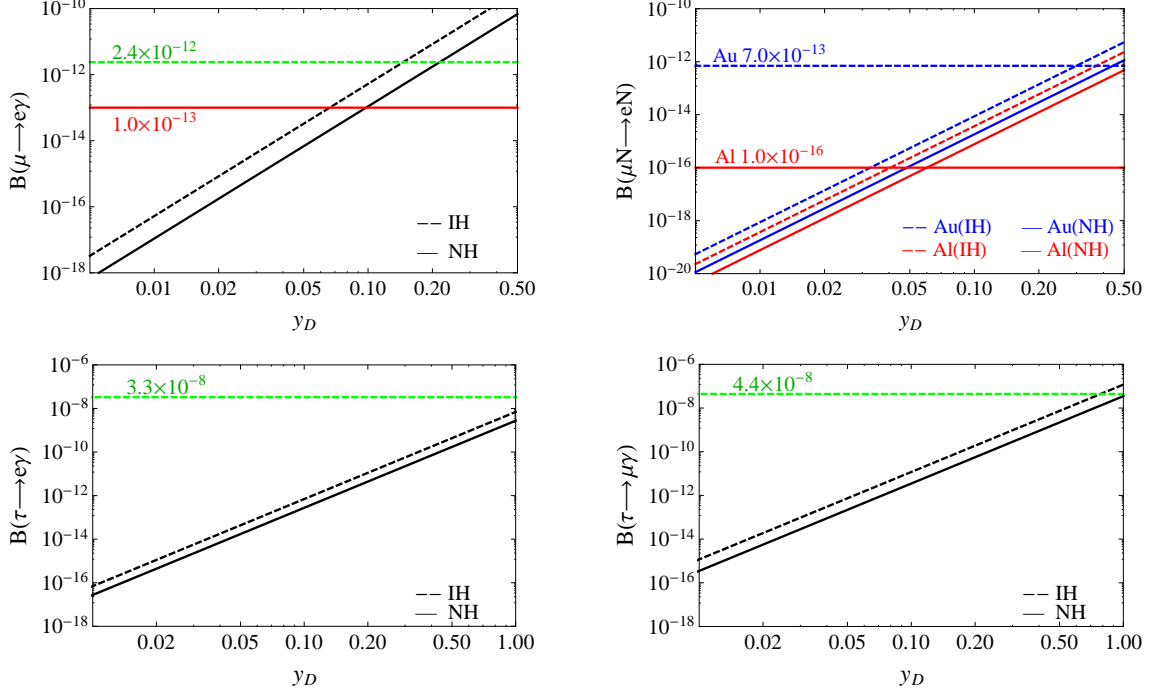


FIG. 4: Figures on the top show constraints on  $y_D$  from  $B(\mu \rightarrow e\gamma)$  and  $\mu - e$  conversion rate with current bound (dashed line) and future sensitivity (solid line) for normal(solid line) and inverted(dashed line) hierarchy. Figures at the bottom show constraints on  $y_D$  from  $\tau \rightarrow e\gamma$  (left) and  $\tau \rightarrow \mu\gamma$  (right).

The constraints on  $y_D$  are shown in Fig.4. We see that the current upper limits from  $\mu \rightarrow e\gamma$  and  $\mu - e$  conversion using Au can already constrain  $y_D$  to be less than 0.2 and 0.4, respectively. Future  $\mu - e$  conversion experiments can reach a sensitivity of 0.05 on  $y_D$ . The model will be constrained when new data become available. The constraints from  $\tau \rightarrow \mu(e)\gamma$  are weaker.

In the above studies, we have taken some bench mark values to have some ideas about the possibility of observing LFV effects. Our studies show that it is possible to have large observable LFV effects at near future experiment, in particular for  $\mu - e$  conversion experiments. We, however, should note that from such studies it is not possible to rule out the model because the allowed parameters can have large or small LFV effect. For example, for neutrino mass generation, the scale of neutrino mass depends on  $y_D \times \lambda_{\Delta\sigma H}$ , but  $\lambda_{\Delta\sigma H}$  does not show up directly in the leading LFV effects which we have studied. Even assuming all other relevant parameters are fixed in the model, by adjusting the size of  $\lambda_{\Delta\sigma H}$  one can have



different values of  $y_D$  to satisfy constraint on  $y_D$  from LFV processes. There are some other processes which can provide additional tests for the model. We find that the correlation of  $h \rightarrow \gamma\gamma$  and  $h \rightarrow \gamma Z$  can be a good indicator. We will discuss this later.

In the above studies, the new physics scale is set by the masses of particles in the  $D$  doublet. We now briefly discuss LHC signature of these particles.  $D^0\bar{D}^0$ ,  $D^0D^-$  and  $D^-D^+$  can be pair produced through  $Z$ ,  $W^-$ ,  $\gamma$  and  $Z$  s-channel exchanges with the cross sections of order  $\mathcal{O}(10)$  fb for mass  $m_D$  around 500 GeV.

For  $D^0\bar{D}^0$  production, since  $D^0$  decays into  $\nu S$ , the signature is missing energy which would be similar to dark matter signature with photon or gluon emissions from the initial quark. The final state is thus a high- $p_T$  photon/gluon and missing energy. Detections of dark matter pair production processes from CMS[21] and ATLAS[22] have been performed. As no excess from SM predictions observed in both experiments, constraints on dark matter mass can then be given accordingly for pair production of dark matter candidates[23]. The current data cannot rule out  $D^0$  of order a few hundred GeV.

$D^-$  will decay into  $l^- S$ . The pair production of  $D^0D^-$  through  $W^-$  exchange can be searched by  $pp \rightarrow l^- + E_T + X$ . There will be SM background from  $W^- \rightarrow l^- \bar{\nu}$  and  $W^- Z/W^- \rightarrow l^- \bar{\nu} \nu$ . Additionally,  $W^+W^-$  production with leptonic decays will also have a possibility to be background when one charged lepton (here  $l^+$ ) is too soft or too forward. To optimize the signal from these backgrounds, one can impose  $p_T^l$  cut on charged lepton. With 8 TeV energy at the LHC and  $20fb^{-1}$ , it is difficult to cut down the background to have enough signal events. We find that it is possible to achieve a discovery level at  $5\sigma$  for 14 TeV center of mass frame energy with  $300fb^{-1}$ . In Table I, we show the cross section with a selective cut of  $p_T^l > 120$  GeV. We have chosen the cut for  $p_T^l$  so that the signal can be established at  $5\sigma$  level statistically. With a higher cut for  $p_T^l$ , one can have a higher significance level, but the event number will be smaller. With this cut of  $p_T^l$  the signal is slightly eliminated while the backgrounds are effectively suppressed. Note that, in the calculation of signal, we have taken the  $D$  doublets with almost degenerate masses and used the bench mark values given before. In the narrow width approximation, the cross section for  $l$  charged lepton in the final state is proportional to  $\sum_i (Y_D^{li} Y_D^{li*} / \sum_l Y_D^{li} Y_D^{li*})$  for degenerate  $D_i$ . The cross section for  $pp \rightarrow l^- + E_T + X$ , therefore, is almost independent of  $y_D$ . The pair production of  $D^-D^+$  will have the signal  $l^-l^+$  plus missing energies. Since there are two leptons in the final state, the analysis is more involved. We will not discuss

this here. The numbers in Table I show that with an integrated luminosity of  $300\text{fb}^{-1}$  for centre-of-mass energy at 14 TeV, for both normal and inverted hierarchy cases, signal of  $5\sigma$  significance can be achieved using  $pp \rightarrow l^- + E_T^l + X$ . It is interesting to carry out such a search.

	Signal [fb](NH and IH)		Background[fb]		
	$\sigma(pp \rightarrow D^0 Sl^-)$		$\sigma(W^- \rightarrow l^- \bar{\nu})$	$\sigma(W^- Z/W^- \rightarrow l^- \bar{\nu} \nu \bar{\nu})$	$\sigma(W^+ W^-)$
14 TeV	11.1	14.2	$8.67 \times 10^6$	345.3	1856
$p_T^l > 120$ GeV	9.66	12.3	1080	6.78	26

TABLE I: Cross sections of signal with  $m_D = 500\text{GeV}$  and  $m_S = 150$  GeV and corresponding backgrounds. In both signal and backgrounds, charged lepton of  $e^-$  and  $\mu^-$  are included.

#### IV. $h \rightarrow \gamma\gamma$

There are strong indications from LHC that the Higgs particle has been discovered with a mass of 126 GeV whose couplings to gauge bosons are consistent with SM Higgs, but with an enhanced  $h \rightarrow \gamma\gamma$  branching ratio. The experimental value[11] for this channel is  $1.8 \pm 0.5$  (ATLAS) ( $1.56 \pm 0.43$ (CMS)) times that predicted by the SM. Recently ATLAS has updated their result with[24]  $1.8 \pm 0.3(\text{stat.})_{-0.15}^{+0.21}(\text{sys.})_{-0.14}^{+0.20}(\text{theory})$  times the value predicted by the SM. The central value is higher than the SM prediction. If confirmed, new physics beyond the SM is required to explain it. In the model we are studying, this can be explained by new contribution from charged particles in the triplet scalar  $\Delta$  with relatively low mass coupled to the usual Higgs boson at loop levels. We now discuss how enhancement can be achieved. There have been extensive studies for similar triplet scalar contributions to  $h \rightarrow \gamma\gamma$ [25, 26]. Our study is more model inspired, the triplet does not have non-zero vev, and also the  $\Delta$  does not decay into pure SM particles. The LHC signatures for  $\Delta$  particles are different than other models.

In the model we are considering, electroweak symmetry breaking is induced by the non-zero vev of Higgs doublet  $H = (h^+, (v + h + iI)/\sqrt{2})^T$ . The charged  $h^+$  and the neutral fields  $I$  are “eaten” by  $W$  and  $Z$ . The  $h$  is the physical Higgs field similar to the one in SM. Since this is the only field having a non-zero vev in the theory, at the tree level, the Higgs  $h$  couplings to gauge bosons are the same as those in the SM. The Yukawa couplings

to SM fermions also have the same form as those in the SM. At one loop level, deviations start to show up. A particularly interesting one is modification for  $h \rightarrow \gamma\gamma$  coupling, due to the existence of new charged particles  $\Delta^{-,--}$  and their non-zero couplings to  $h$ . Note that the new particles, do not have strong interactions, the process  $gg \rightarrow h$  is not affected to the lowest order. So the model will not alter the production rate of  $h$  predicted by the SM to the leading order in agreement with data.

The couplings of  $h$  to  $\Delta^{-,--}$  come from  $\lambda_{H\Delta}^{1,2}(\Delta^\dagger\Delta H^\dagger H)_{1,2}$  after  $H$  develops vev. The  $h\bar{\Delta}\Delta$  couplings are given by

$$L \sim -[\lambda_{\Delta H}^1(\Delta^+\Delta^- + \Delta^{++}\Delta^{--}) + \lambda_{\Delta H}^2(\Delta^{++}\Delta^{--} + \frac{1}{2}\Delta^+\Delta^-)]vh. \quad (16)$$

Combined with contributions from  $W$  and top in the loop, the  $h \rightarrow \gamma\gamma$  rate is modified by a factor  $R_{\gamma\gamma} = \Gamma(h \rightarrow \gamma\gamma)_{U(1)_D}/\Gamma(h \rightarrow \gamma\gamma)_{\text{SM}}$  given by

$$R_{\gamma\gamma} = |1 + \frac{v^2}{2} \frac{1}{A_1(\tau_W) + N_c Q_t^2 A_{1/2}(\tau_t)} \left\{ \frac{\lambda_{H\Delta}^1 + \frac{1}{2}\lambda_{H\Delta}^2}{m_{\Delta^-}^2} A_0(\tau_{\Delta^-}) + \frac{4(\lambda_{H\Delta}^1 + \lambda_{H\Delta}^2)}{m_{\Delta^{--}}^2} A_0(\tau_{\Delta^{--}}) \right\}|^2 \quad (17)$$

where  $\tau_i \equiv (m_h^2/4m_i^2)$ ,  $i = t, W, \Delta^-$  and  $\Delta^{--}$ .  $N_c$  is the degree freedom of color and  $Q_t$  is the charge of top quark.  $A_1(\tau_W)$  and  $A_{1/2}(\tau_t)$  come from SM  $W$  boson and top quark contributions.  $A_0(\tau_\Delta)$  comes from new scalars in the model. They are given by

$$\begin{aligned} A_0(x) &= -x^{-2}[x - f(x)]; A_{1/2}(x) = 2x^{-2}[x + (x-1)f(x)]; \\ A_1(x) &= -x^{-2}[2x^2 + 3x + 3(2x-1)f(x)]; \\ f(x) &= \begin{cases} \arcsin^2 \sqrt{x}, & x \geq 1 \\ -\frac{1}{4}[\ln \frac{1+\sqrt{1-x^{-1}}}{1-\sqrt{1-x^{-1}}} - i\pi]^2, & x < 1 \end{cases} \end{aligned} \quad (18)$$

Eq.(17) tells that new contributions to the ratio  $R_{\gamma\gamma}$  depend on not only the couplings  $\lambda_{H\Delta}^{1,2}$ , but also the masses of the charged scalars. The scalar masses depend on several parameters. Neglecting the mixing between  $\sigma$  and  $\Delta^0$ , the component fields in  $\Delta$  masses are given by

$$\begin{aligned} m_{\Delta^0}^2 &= \mu_\Delta^2 + \frac{1}{2}\lambda_{H\Delta}^1 v^2, \\ m_{\Delta^-}^2 &= \mu_\Delta^2 + \frac{1}{2}\lambda_{H\Delta}^1 v^2 + \frac{1}{4}\lambda_{H\Delta}^2 v^2, \\ m_{\Delta^{--}}^2 &= \mu_\Delta^2 + \frac{1}{2}\lambda_{H\Delta}^1 v^2 + \frac{1}{2}\lambda_{H\Delta}^2 v^2, \end{aligned} \quad (19)$$

To see how the model can enhance the  $h \rightarrow \gamma\gamma$  to be consistent with LHC data, we will keep the  $\Delta^0$  mass to be  $m_{\Delta^0} = 300$  GeV as used in the discussions on the neutrino masses and vary  $\lambda_{H\Delta}^{1,2}$  to obtain the new contributions to  $R_{\gamma\gamma}$ . The results are shown in Fig.5 and Fig.6.

We also calculated new contributions to  $h \rightarrow \gamma Z$ . We confirm the formalisms in Ref[26]. Using these formulas, we obtain the ratio of  $h \rightarrow \gamma Z$  in the  $U(1)_D$  model to that of SM as

$$R_{Z\gamma} = \left| 1 - \frac{2v}{A_{SM}^{Z\gamma}} \left\{ \frac{g_{Z\Delta^-\Delta^-}(\lambda_{H\Delta}^1 + \frac{1}{2}\lambda_{H\Delta}^2)}{m_{\Delta^-}^2} A_0(z_{\Delta^-}, \lambda_{\Delta^-}) + \frac{2g_{Z\Delta^-\Delta^{--}}(\lambda_{H\Delta}^1 + \lambda_{H\Delta}^2)}{m_{\Delta^{--}}^2} A_0(z_{\Delta^{--}}, \lambda_{\Delta^{--}}) \right\} \right|^2 \quad (20)$$

where  $z_i = 4m_i^2/m_h^2$ ,  $\lambda_i \equiv 4m_i^2/m_Z^2$  and  $g_{Z\Delta\Delta} \equiv (T_\Delta^3 - Q_\Delta s_W^2)/s_W c_W$ .  $A_{SM}^{Z\gamma}$  comes from SM W boson and top quark contributions and  $A_0$  comes from new charged scalars in this model. They are given by

$$\begin{aligned} A_{SM} &= \frac{2}{v} \left[ \cot \theta_W A_1(z_W, \lambda_W) + N_c \frac{2Q_t(T_3^t - 2Q_t s_W^2)}{s_W c_W} A_{1/2}(z_t, \lambda_t) \right], \\ A_0(x, y) &= I_1(x, y), \\ A_{1/2}(x, y) &= I_1(x, y) - I_2(x, y), \\ A_1(x, y) &= 4(3 - \tan^2 \theta_W) I_2(x, y) + [(1 + 2x^{-1}) \tan^2 \theta_W - (5 + 2x^{-1})] I_1(x, y), \end{aligned}$$

where  $T_3^t$  is the third component of isospin of top quark, and  $I_1, I_2$  are given by

$$\begin{aligned} I_1(x, y) &= \frac{xy}{2(x-y)} + \frac{x^2 y^2}{2(x-y)^2} [f(x^{-1}) - f(y^{-1})] + \frac{x^2 y}{(x-y)^2} [g(x^{-1}) - g(y^{-1})], \\ I_2(x, y) &= -\frac{xy}{2(x-y)} [f(x^{-1}) - f(y^{-1})], \\ g(x) &= \sqrt{x^{-1} - 1} \arcsin \sqrt{x}. \end{aligned}$$

In the allowed  $\lambda_{H\Delta}^i$  space,  $h \rightarrow \gamma Z$  will be modified significantly. We show the predicted scaling factor  $R_{\gamma Z} = \Gamma(h \rightarrow \gamma Z)_{U(1)_D} / \Gamma(h \rightarrow \gamma Z)_{SM}$  in Fig.7 and Fig.8.

To enhance the ratio  $R_{\gamma\gamma}$ , negative  $\lambda_{H\Delta}^{1,2}$  are preferred. With fixed  $m_{\Delta^0}$ , negative  $\lambda_{H\Delta}^2$  implies that  $m_{\Delta^0} > m_{\Delta^-} > m_{\Delta^{--}}$ . From Fig.5, we can see that with negative  $\lambda_{H\Delta}^{1,2}$  of order  $\mathcal{O}(1)$ , the ATLAS and CMS results on  $h \rightarrow \gamma\gamma$  can be reproduced. If one controls the magnitude of  $\lambda_{H\Delta}^{1,2}$  as small as possible from perturbation consideration, the optimal values for  $\lambda_{H\Delta}^{1,2}$  are around  $-0.8$  and  $-0.6$ , respectively. With these values,  $\Delta^-$  and  $\Delta^{--}$  masses are given by 284.5 GeV and 268 GeV. More negative  $\lambda_{H\Delta}^2$  will make the mass of  $\Delta^{--}$  smaller

which may be in conflict with LHC data. We should take  $|\lambda_{H\Delta}^2|$  as small as possible. With the same parameters, the predicted value for  $R_{\gamma Z}$  are shown in Fig.7.

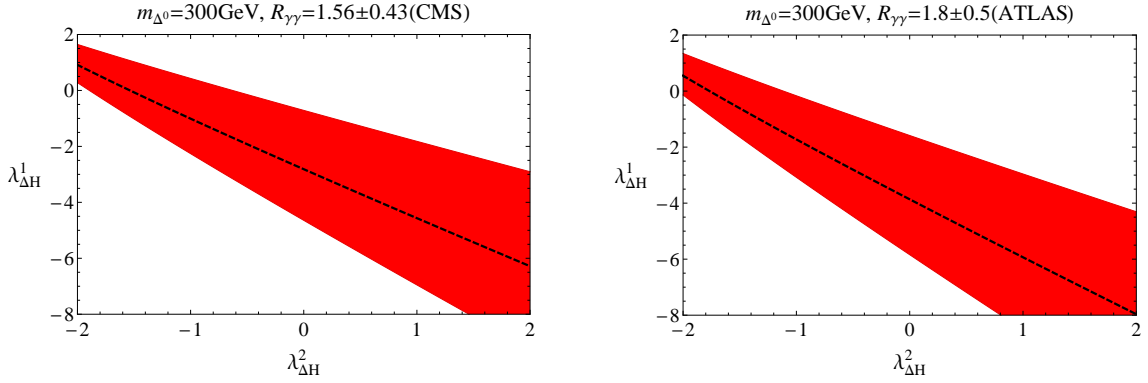


FIG. 5: Constraints on  $\lambda_{H\Delta}^1$  and  $\lambda_{H\Delta}^2$  with  $m_{\Delta^0} = 300\text{GeV}$ .

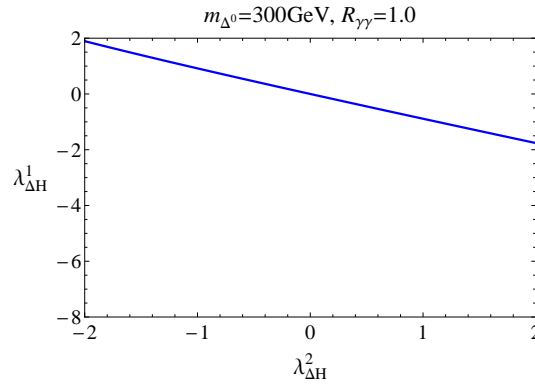


FIG. 6: Constraints on  $\lambda_{H\Delta}^1$  and  $\lambda_{H\Delta}^2$  with  $R_{\gamma\gamma} = 1$  for  $m_{\Delta^0} = 300\text{GeV}$ .

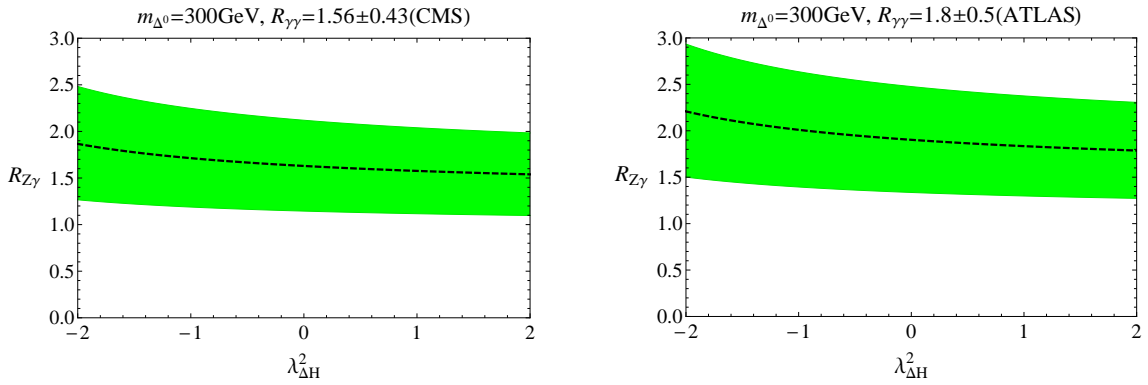


FIG. 7: Scaling factor for  $h \rightarrow Z\gamma$  with the same parameters for  $h \rightarrow \gamma\gamma$ .

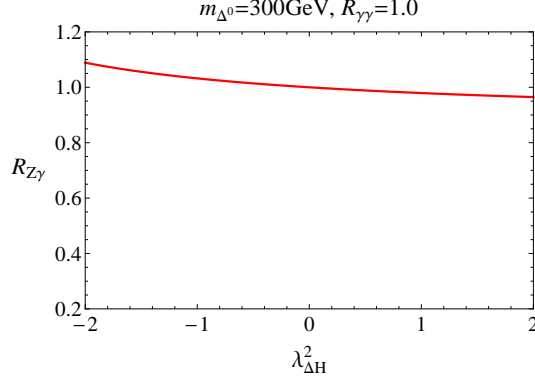


FIG. 8: Scaling factor for  $h \rightarrow Z\gamma$  with the same parameters for  $R_{\gamma\gamma} = 1$ .

With  $\lambda_{H\Delta}^2 > 0$ , the mass hierarchy for the component fields in the triplet is  $m_{\Delta^0} < m_{\Delta^-} < m_{\Delta^{--}}$ . In this case, the new contributions may cancel out if  $\lambda_{H\Delta}^1$  is kept negative. We demonstrate this possibility in Fig.6, where  $R_{\gamma\gamma}$  is kept to be 1. For this parameter space, the predicted  $R_{\gamma Z}$  is shown in Fig.8.

In general there is a correlation between  $h \rightarrow \gamma\gamma$  and  $h \rightarrow \gamma Z$ , that is, enhancement of  $h \rightarrow \gamma\gamma$  leads to an enhanced  $h \rightarrow \gamma Z$ . This fact may be used as a test for this model. Should an anti-correlation between  $h \rightarrow \gamma\gamma$  and  $h \rightarrow \gamma Z$  will be confirmed, this model will be in trouble. But even if  $h \rightarrow \gamma\gamma$  agrees with SM prediction,  $h \rightarrow \gamma Z$  can be different as can be seen in Fig.8.

Our analysis show that in order to explain the possible enhanced  $h \rightarrow \gamma\gamma$ , negative  $\lambda_{H\Delta}^{1,2}$  of order minus one is needed. If the current data at the LHC will be further confirmed, we need to check if the required negative  $\lambda_{H\Delta}^{1,2}$  are consistent with other constraints. One of the constraints is from the stability of Higgs potential. Here we argue that this is not a problem.

Potential bounded from below concerns potentials at fields taking large values. Let us consider terms involving  $\lambda_H$ ,  $\lambda_{\Delta}^{1,2}$ , and  $\lambda_{H\Delta}^{1,2}$  in the case where  $S$  and  $\sigma$  fields are absent and carry out an similar analysis as in Ref.[27]. At large values of  $H$  and  $\Delta$ , the potential is given by

$$\lambda_H x^2 + (\lambda_{\Delta}^1 + \lambda_{\Delta}^2 \eta) y^2 + (\lambda_{H\Delta}^1 + \lambda_{H\Delta}^2 \xi) xy, \quad (21)$$

where  $x = H^\dagger H$ ,  $y = Tr(\Delta^\dagger \Delta)$ ,  $\eta = Tr(\Delta^\dagger \Delta \Delta^\dagger \Delta) / (Tr(\Delta^\dagger \Delta))^2$ , and  $\xi = (H^\dagger \Delta \Delta^\dagger H) / (H^\dagger H Tr(\Delta^\dagger \Delta))$ . The ranges for  $\eta$  and  $\xi$  are  $1/2 \sim 1$  and  $0 \sim 1$ , respectively.

By definition both  $x$  and  $y$  are larger than zero. To satisfy Eq. (21),  $\lambda_H$  and  $(\lambda_{\Delta}^1 + \lambda_{\Delta}^2 \eta)$  must be positive. If  $(\lambda_{H\Delta}^1 + \lambda_{H\Delta}^2 \xi)$  is larger than zero, Eq. (21) is satisfied.

For  $(\lambda_{H\Delta}^1 + \lambda_{H\Delta}^2 \xi) < 0$  the conditions are different. This is the case if we use enhanced  $R_{\gamma\gamma}$  to explain the data, it is required that both  $\lambda_{H\Delta}^{1,2}$  to be negative are preferred. In the following we study this case. The positivity conditions can be obtained by requiring the diagonal elements and the determinant of the following matrix to be positive

$$M_p = \begin{pmatrix} \lambda_H & (\lambda_{H\Delta}^1 + \lambda_{H\Delta}^2 \xi)/2 \\ (\lambda_{H\Delta}^1 + \lambda_{H\Delta}^2 \xi)/2 & \lambda_\Delta^1 + \lambda_\Delta^2 \eta \end{pmatrix}. \quad (22)$$

Without the conditions  $\lambda_{H\Delta}^1 < 0$ ,  $\lambda_{H\Delta}^2 < 0$ ,  $x > 0$ , and  $y > 0$ , the parameters need to simultaneously satisfy

$$\begin{aligned} \lambda_H > 0, \quad \lambda_\Delta^1 + \lambda_\Delta^2 > 0, \quad \lambda_\Delta^1 + \frac{1}{2}\lambda_\Delta^2 > 0, \\ \lambda_H(\lambda_\Delta^1 + \lambda_\Delta^2) > \frac{1}{4}(\lambda_{H\Delta}^1)^2, \quad \lambda_H(\lambda_\Delta^1 + \lambda_\Delta^2) > \frac{1}{4}(\lambda_{H\Delta}^1 + \lambda_{H\Delta}^2)^2, \\ \lambda_H(\lambda_\Delta^1 + \frac{1}{2}\lambda_\Delta^2) > \frac{1}{4}(\lambda_{H\Delta}^1)^2, \quad \lambda_H(\lambda_\Delta^1 + \frac{1}{2}\lambda_\Delta^2) > \frac{1}{4}(\lambda_{H\Delta}^1 + \lambda_{H\Delta}^2)^2. \end{aligned} \quad (23)$$

In the above, we have also taken into consideration of the ranges of  $\eta$  and  $\xi$ .

With the conditions  $\lambda_{H\Delta}^1 < 0$ ,  $\lambda_{H\Delta}^2 < 0$ ,  $x > 0$ , and  $y > 0$ , the conditions of positivity for Eq. (21) are relaxed to be

$$\begin{aligned} \lambda_H > 0, \quad \lambda_\Delta^1 + \lambda_\Delta^2 > 0, \quad \lambda_\Delta^1 + \frac{1}{2}\lambda_\Delta^2 > 0, \\ \sqrt{\lambda_H(\lambda_\Delta^1 + \lambda_\Delta^2)} > -\frac{1}{2}\lambda_{H\Delta}^1, \quad \sqrt{\lambda_H(\lambda_\Delta^1 + \lambda_\Delta^2)} > -\frac{1}{2}(\lambda_{H\Delta}^1 + \lambda_{H\Delta}^2), \\ \sqrt{\lambda_H(\lambda_\Delta^1 + \frac{1}{2}\lambda_\Delta^2)} > -\frac{1}{2}\lambda_{H\Delta}^1, \quad \sqrt{\lambda_H(\lambda_\Delta^1 + \frac{1}{2}\lambda_\Delta^2)} > -\frac{1}{2}(\lambda_{H\Delta}^1 + \lambda_{H\Delta}^2). \end{aligned} \quad (24)$$

A Higgs mass of 125 GeV, implies  $\lambda_H = 0.13$ . Our required  $\lambda_{H\Delta}^{1,2}$  of order minus one and the above conditions can be satisfied if one chooses both  $\lambda_\Delta^{1,2}$  to be positive and satisfy  $\lambda_\Delta^1 + \frac{1}{2}\lambda_\Delta^2 > 1/\lambda_H = 7.7$  (with  $\lambda_{H\Delta}^{1,2} = -1.0$ ). This condition can be easily satisfied by choosing  $\lambda_\Delta^{1,2}$  to be about 5 which are well below the unitarity bounds on  $\lambda_\Delta^{1,2}$  of order  $4\pi$ [27].

Our model is more complicated because there are also  $S$  and  $\sigma$  fields. The term proportional to  $\lambda_{\Delta\sigma H}$  can be chosen to be small and neglected. The corresponding  $M_p$  matrix becomes a  $4 \times 4$  one. The conditions for potential bounded from below require the diagonal elements, the determinant of the matrix, and all determinants of its sub-matrices to be positive with the constraints for variables similar to  $x$  and  $y$  to be positive. The conditions for potential bounded from below include the ones discussed above, but have some additional

ones. For our purpose, we need to fix  $\lambda_H$  to be 0.13, and  $\lambda_{H\Delta}^{1,2}$  to be around -1.0 to satisfy the positive conditions. Since several new independent parameters  $\lambda_{S,\sigma,H\sigma,HS,\Delta S,\Delta\sigma,\Delta S}$  come into play, one is able to find reasonable parameter spaces to satisfy the conditions. For example, with  $\lambda_{S,\sigma} > 0$ ,  $\lambda_{H\sigma,\Delta S,\Delta\sigma,\Delta S}$  to be zero. If one requires  $S$  to play the role of dark matter,  $\lambda_{HS}$  should not be zero [5]. There is a large range for  $\lambda_{HS}$  below 0.03 which can satisfy dark matter constraint for dark matter mass around half of Higgs mass and larger than 130 GeV [5]. The positivity of potential at large values of fields can be satisfied.

Before closing this section, we make some comments about effects of the  $\Delta$  particle at the LHC. In the case with  $\lambda_{H\Delta}^2 < 0$ ,  $\Delta^{--}$  is the lightest particle in the  $\Delta$  triplet. It is stable in the scenario where  $2m_S$  mass is larger than  $\Delta$  mass, that is,  $\Delta^{--} \rightarrow D^- D^- \rightarrow l^- Sl^- S$  is kinematically forbidden. This is the case for the bench mark values we are using. With a mass of order a few hundred GeV,  $\Delta^{--}$  can be produced at the LHC with a cross section of order about 10 fb. Although it does not decay into SM particles making the direct detection difficult, being a stable heavy charged particle it does leave tracks in the detector which have been searched for at the LHC. The current data from LHC still allow mass of order a few GeV[28]. If it turns out that  $\Delta^{--}$  mass is large enough, and  $\Delta^{--} \rightarrow D^- D^- \rightarrow l^- Sl^- S$  becomes kinematically possible, then  $l^- l^- + E_T +$  jets is the signal to search. This has small SM background and can be searched at the LHC.

In the case with  $\lambda_{H\Delta}^2 > 0$ ,  $\Delta^0$  is the lightest particle in the  $\Delta$  triplet. It can also be copiously produced at the LHC because the mass can be as low as a few hundred GeV. Search for this particle is similar to search for dark matter which can annihilate into quarks. Some of the processes which can provide information about this particle are single photon plus missing energy and mono-jet plus missing energy. ATLAS and CMS experiments at the LHC have carried out such studies. At this moment the data are not constraining enough to rule out the parameter space we are using[21–23]. But as more data become available, the model can be constrained more.

## V. CONCLUSIONS

We have studied some phenomenological consequences of a two loop radiative inverse seesaw model with an unbroken global  $U(1)_D$  symmetry. This model has a natural candidate for dark matter which allows larger Yukawa couplings and low mass of order a hundred GeV



charged new particles in the triplet scalar  $\Delta$ . The large Yukawa couplings can lead to large leptonic flavor changing effects in  $\mu \rightarrow e\gamma$  and  $\mu - e$  conversion. The current data have already constrained the size of the allowed Yukawa couplings. Future improved experiments on  $\mu - e$  conversion can improve the constraint by several orders of magnitude. The existence of low mass charged particle in the triplet  $\Delta$  make it possible to enhance the  $h \rightarrow \gamma\gamma$  to explain the deviation between the LHC data and SM prediction.

### Acknowledgments

This work was supported in part by NSC of ROC, and NNSF(grant No:11175115) and Shanghai science and technology commission (grant No: 11DZ2260700) of PRC.

- 
- [1] P. Minkowski, Phys. Lett. B **67**, 421 (1977); T. Yanagida, in *Workshop on Unified Theories*, KEK report 79-18 p.95 (1979); M. Gell-Mann, P. Ramond, R. Slansky, in *Supergravity* (North Holland, Amsterdam, 1979) eds. P. van Nieuwenhuizen, D. Freedman, p.315; S. L. Glashow, in *1979 Cargese Summer Institute on Quarks and Leptons* (Plenum Press, New York, 1980) eds. M. Levy, J.-L. Basdevant, D. Speiser, J. Weyers, R. Gastmans and M. Jacobs, p.687; R. N. Mohapatra and G. Senjanovic, Phys. Rev. Lett. **44**, 912 (1980).
- [2] W. Konetschny and W. Kummer, Phys. Lett. B **70**, 433 (1977); T. P. Cheng and L. F. Li, Phys. Rev. D **22**, 2860 (1980); J. Schechter and J. W. F. Valle, Phys. Rev. D **22**, 2227 (1980); G. Lazarides, Q. Shafi and C. Wetterich, Nucl. Phys. B **181**, 287 (1981); R. N. Mohapatra and G. Senjanovic, Phys. Rev. D **23**, 165 (1981); R. Barbieri, D. V. Nanopoulos, G. Morchio and F. Strocchi, Phys. Lett. B **90**, 91 (1980).
- [3] R. Foot, H. Lew, X. G. He and G. C. Joshi, Z. Phys. C **44**, 441 (1989).
- [4] R.N. Mohapatra, Phys. Rev. Lett. **56**, 561(1986); R.N. Mohapatra and J. W. F. Valle, Phys. Rev. **D34**, 1642(1986).
- [5] G. Guo, X.G. He and G.N. Li, JHEP **1210**, 044 (2012) [arXiv:1207.6308[hep-ph]]
- [6] E. Komatsu et al. [WMAP Collaboration], Astrophys. J. Suppl. **192**, 18(2011).
- [7] V. Silveira and A. Zee, Phys. Lett. B **161**, 136 (1985);

- [8] C.P. Burgess, M. Pospelov, and T. ter Veldhuis, Nucl. Phys. B **619**, 709 (2001) [arXiv:hep-ph/0011335]; X.G. He, S.Y. Ho, J. Tandean, and H.C. Tsai, Phys. Rev. D **82**, 035016 (2010) [arXiv:1004.3464 [hep-ph]]; X.G. He, T. Li, X.Q. Li, J. Tandean, and H.C. Tsai, Phys. Rev. D **79**, 023521 (2009) [arXiv:0811.0658 [hep-ph]]; X.G. He, T. Li, X.Q. Li, and H.C. Tsai, Mod. Phys. Lett. A **22**, 2121 (2007) [arXiv:hep-ph/0701156]; M. Aoki, S. Kane-mura, and O. Seto, Phys. Lett. B **685**, 313 (2010) [arXiv:0912.5536 [hep-ph]]; Y. Cai, X.G. He, and B. Ren, Phys. Rev. D **83**, 083524 (2011) [arXiv:1102.1522 [hep-ph]]. X.G. He and J. Tandean, Phys. Rev. D **84**, 075018 (2011) [arXiv:1109.1277 [hep-ph]]; X. -G. He, B. Ren and J. Tandean, Phys. Rev. D **85**, 093019 (2012) [arXiv:1112.6364 [hep-ph]].
- [9] K. Cheung, Y. -L. S. Tsai, P. -Y. Tseng, T. -C. Yuan and A. Zee, JCAP **1210**, 042 (2012) [arXiv:1207.4930 [hep-ph]].
- [10] J. McDonald, Phys. Rev. D **50**, 3637 (1994) [arXiv:hep-ph/0702143].
- [11] G. Aad *et al.* [ATLAS Collaboration], arXiv:1207.7214 [hep-ex]; S. Chatrchyan *et al.* [CMS Collaboration] , Phys. Lett. B **716**, 30 (2012).
- [12] G. L. Fogli, E. Lisi, A. Marrone, D. Montanino, A. Palazzo and A. M. Rotunno, arXiv:1205.5254 [hep-ph].
- [13] R. Kitano, M. Koike and Y. Okada, Phys. Rev. D **66**, 096002 (2002) [Erratum-ibid. D **76**, 059902 (2007)].
- [14] N. Deshpande, T. Enkhbat, T. Fukuyama, X. G. He, L. H. Tsai and K. Tsumura, [arXiv:1106.5085 [hep-ph]].
- [15] J. Adam *et al.*, MEG Collaboration, [arXiv:1107.5547].
- [16] Research Proposal to INFN, “The MEG experiment: search for the  $\mu^+ \rightarrow e^+\gamma$  decay at PSI”, September 2002.
- [17] J. Beringer *et al.*(Particle Data Group), Phys. Rev. D **86**, 010001 (2012).
- [18] W. H. Bertl *et al.*, [SINDRUM II Collaboration], Eur. Phys. J. C **47**, 337 (2006).
- [19] J. P. Miller [Mu2E collaboration], *Proposal to Search for  $\mu^- N \rightarrow e^- N$  with a Single Event Sensitivity Below  $10^{-16}$* .
- [20] Y. Kuno *et al.*, [COMET collaboration], *An Experimental Search for lepton Flavor Violating  $\mu - e$  Conversion at Sensitivity of  $10^{-16}$  with a Slow-Extracted Bunched Beam*.
- [21] S. Chatrchyan *et al.* [CMS Collaboration], Phys. Rev. Lett. **108**, 261803 (2012) [arXiv:1204.0821 [hep-ex]]; S. Chatrchyan *et al.* [CMS Collaboration], JHEP **1209**, 094 (2012)

- [arXiv:1206.5663 [hep-ex]].
- [22] G. Aad *et al.* [ATLAS Collaboration], arXiv:1209.4625 [hep-ex]; [ATLAS Collaboration], ATLAS-CONF-2012-084.
- [23] see e.g., J. Goodman, M. Ibe, A. Rajaraman, W. Shepherd, T. M. P. Tait and H. -B. Yu, Phys. Rev. D **82**, 116010 (2010) [arXiv:1008.1783 [hep-ph]]; P. J. Fox, R. Harnik, J. Kopp and Y. Tsai, Phys. Rev. D **85**, 056011 (2012) [arXiv:1109.4398 [hep-ph]].
- [24] G. Aad *et al.* [ATLAS Collaboration], ATLAS-CONF-2012-168.
- [25] A. Arhrib, R. Benbrik, M. Chabab, G.Moultaka and L. Rahili, JHEP **1204**, 136 (2012) [arXiv:1112.5453 [hep-ph]]; A. Arhrib, R. Benbrik, M. Chabab, G.Moultaka and L. Rahili, arXiv:1202.6621 [hep-ph]; A. G. Akeroyd and S. Moretti, Phys. Rev. D **86**, 035015 (2012) [arXiv:1206.0535 [hep-ph]]; C. -W. Chiang and K. Yagyu, arXiv:1207.1065 [hep-ph]; Mikael Chala, arXiv:1210.6208 [hep-ph]; Ivica Picek and Branimir Radovčić, arXiv:1210.6449 [hep-ph]; E. J. Chun, H. M. Lee and P. Sharma, JHEP **1211**, 106 (2012) [arXiv:1209.1303 [hep-ph]].
- [26] C. -S. Chen, C. -Q. Geng, D. Huang and L. -H. Tsai, arXiv:1301.4694 [hep-ph]; C. -S. Chen, C. -Q. Geng, D. Huang and L. -H. Tsai, arXiv:1302.0502 [hep-ph].
- [27] A. Arhrib, R. Benbrik, M. Chabab, G. Moultaka, M. C. Peyranere, L. Rahili and J. Ramadan, Phys. Rev. D **84**, 095005 (2011) [arXiv:1105.1925 [hep-ph]].
- [28] G. Aad *et al.* [ATLAS Collaboration], arXiv:1106.4495[hep-ex]; S. Chatrchyan *et al.* [CMS Collaboration], arXiv: 1205.0272[hep-ex].